

The influence of electrodes on the frequency–temperature characteristics of rotated Y-cut quartz resonators

J. Zelenka *

Electrical Engineering Department, Technical University of Liberec, Hálkova 6, CZ-461 17 Liberec 1, Czech Republic

Received 14 September 1995

Abstract

The incremental two-dimensional equation of motion for small amplitude waves superposed on the homogeneous thermal strain are used for the theoretical description of the influence of the elastic stiffnesses and inertia of electrodes on the frequency–temperature characteristics of the fundamental thickness-shear vibration of the rotated Y-cut quartz resonators. The resonators are considered in the shape of the strip bounded in the X axis direction of the quartz crystal and fully covered on the faces perpendicular to the thickness direction by conducting electrodes. The piezoelectric properties of a quartz plate are neglected. The theoretically obtained results are compared with the measured frequency–temperature characteristics of the AT- and BT-cut quartz plates. © 1997 Elsevier Science B.V.

Keywords: Quartz resonators; Quartz plate vibration; Frequency–temperature characteristics; AT-cut resonators

1. Introduction

The influence of electrodes deposited on the surface of quartz plates on the frequency–temperature characteristics of the quartz plates was studied namely by Tiersten and Sinha [1], Stevens and Tiersten [2] and Sherman [3] during the last eight years. They considered the influence of the thermal stresses induced by the change of the temperature in the piezoelectric plate with thin films covered the surface of the plate and the influence of the energy trapping. In the present paper the influence of the changes of the inertia and the elastic properties of electrodes caused by the change of the temperature on the frequency–temperature characteristic of the electrode quartz resonators are considered.

The linear elastic equations for small vibrations superposed on the thermally induced deformation by steady and uniform temperature changes are used for the description of the influence of electrodes on the frequency–temperature characteristic of the fundamental thickness-shear vibration of rotated Y-cut quartz resonators in the paper. The two-dimensional piezoelectric plate equations based on the Mindlin's power series expansion [4] and the Mindlin's [5] and Tiersten's [6] two-dimensional equations for the plating are used for

the description of the vibration of the fully plated strips. The influence of the temperature changes is included in the description of the vibration by using the incremental two-dimensional equations of motion derived by Lee and Yong [7]. The piezoelectric properties of the plate are neglected.

The influence of electrodes on the frequency–temperature characteristics of AT-cut quartz resonators was computed and compared with the measured frequency–temperature characteristics of quartz resonators with silver and gold electrodes [8]. The thickness of the electrodes of the measured resonators on each side was from 100 to 1000 nm and the resonant frequency of the thickness-shear vibration was approximately 10 MHz.

2. Incremental equations of motion and frequency–temperature equation of unplated rotated Y-cut quartz plate

The rotated Y-cut quartz plate shown with its coordinates and dimensions in Fig. 1 is considered in the subsequent discussion. Following Lee and Yong [7] the influence of the thermally biased homogeneous strain is expressed by means of the term β_{ik} and thermally dependent elastic stiffnesses D_{ijkl} .

* E-mail: jiri.zelenka@vslib.cz; fax: +42 48 27383.

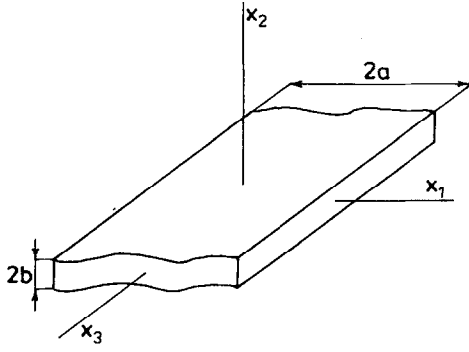


Fig. 1. rotated Y-cut resonator in orthogonal system of axis.

The term β_{ik} is given by the relation

$$\beta_{ik} = \delta_{ik} + \alpha_{ik}^{\theta}, \quad (1)$$

where δ_{ik} is the Kronecker delta and homogeneous thermal strain α_{ik}^{θ} is a function of the n th order thermal expansion coefficients $\alpha_{ik}^{(n)}$ and the temperature change $\theta = T - T_0$:

$$\alpha_{ij}^{\theta} = \alpha_{ij}^{(1)}\theta + \alpha_{ij}^{(2)}\theta^2 + \alpha_{ij}^{(3)}\theta^3. \quad (2)$$

The coefficients $\alpha_{ik}^{(n)}$ were measured and published by Bechmann, Ballato and Lukaszek [9] and corrected by Kosinski, Guallieri and Ballato [10].

The thermally dependent elastic stiffnesses D_{ijkl} are given by the relation

$$D_{ijkl} = C_{ijkl} + D_{ijkl}^{(1)}\theta + D_{ijkl}^{(2)}\theta^2 + D_{ijkl}^{(3)}\theta^3, \quad (3)$$

where

$$D_{ijkl}^{(1)} = C_{ijkl}^{(1)} + C_{ijklmn}\alpha_{mn}^{(1)},$$

$$D_{ijkl}^{(2)} = \frac{1}{2}\tilde{C}_{ijkl}^{(2)} + C_{ijklmn}\alpha_{mn}^{(2)}, \quad (4)$$

$$D_{ijkl}^{(3)} = \frac{1}{6}\tilde{C}_{ijkl}^{(3)} + C_{ijklmn}\alpha_{mn}^{(3)}.$$

C_{ijkl} and C_{ijklmn} are second and third order elastic stiffnesses, while $C_{ijkl}^{(1)}$, $\tilde{C}_{ijkl}^{(2)}$ and $\tilde{C}_{ijkl}^{(3)}$ are respectively the first temperature derivative, second and third effective temperature derivatives of elastic stiffnesses C_{ijkl} . The values of the temperature derivatives were calculated and presented by Lee and Yong [7].

The incremental two-dimensional equations of motion for small amplitude waves superposed on homogeneous strain induced by the change of temperature were derived by Lee and Yong [7] in the form

$$\beta_{ik}t_{kj,j}^{(n)} - n\beta_{ik}t_{k2}^{(n-1)} + \beta_{ik}F_k^{(n)} = \rho \sum_{m=0}^{\infty} A_{mn}\ddot{u}_i^{(m)}, \quad (5)$$

where $t_{kj}^{(n)}$ is the n th order incremental stress defined for the purely elastic plate by the relation

$$t_{kj}^{(m)} = D_{ijkl} \sum_{n=0}^{\infty} A_{mn}e_{kl}^{(n)}, \quad (6)$$

$e_{ij}^{(n)}$ is the n th order incremental strain given by the relation

$$e_{ij}^{(n)} = \frac{1}{2}[\beta_{kj}u_{k,i}^{(n)} + \beta_{ki}u_{k,j}^{(n)} + (n+1)(\beta_{2i}\beta_{kj}u_k^{(n+1)} + \delta_{2j}\beta_{ki}u_k^{(n+1)})]. \quad (7)$$

$F_k^{(n)}$ is the n th order incremental face traction defined by the relation

$$F_k^{(n)} = [x_2^n t_{k2}]_{-b}^{+b} \quad (8)$$

and

$$A_{mn} = \begin{cases} \frac{2b^{m+n+1}}{m+n+1} & \text{when } (m+n) \text{ is even,} \\ 0 & \text{when } (m+n) \text{ is odd.} \end{cases}$$

The infinite series of two-dimensional plate Eq. (5) are truncated by retaining terms of order $n=0$ and $n=1$ only in this paper. The resulting incremental two-dimensional equations of motion after including of the correction factors $\kappa_{(ij)}$ for thickness vibrations [11] are

$$\beta_{ik}t_{kj,j}^{(0)} + \beta_{ik}F_k^{(0)} = 2b\rho\ddot{u}_i^{(0)}, \quad (10)$$

$$\beta_{ik}t_{kj,j}^{(1)} - \beta_{ik}t_{k2}^{(0)} + \beta_{ik}F_k^{(1)} = \frac{2}{3}b^3\rho\ddot{u}_i^{(1)},$$

where

$$t_{ij}^{(0)} = 2b\kappa_{(ij)}\kappa_{(kl)}D_{ijkl}e_{kl}^{(0)},$$

$$t_{ij}^{(1)} = \frac{2}{3}b^3D_{ijkl}e_{kl}^{(1)},$$

$$F_j^{(0)} = [t_{2j}]_{-b}^{+b} = t_{2j}(b) - t_{2j}(-b),$$

$$F_j^{(1)} = [x_2 t_{2j}]_{-b}^{+b} = bt_{2j}(b) - bt_{2j}(-b), \quad (11)$$

$$e_{ij}^{(n)} = \frac{1}{2}[\beta_{kj}u_{k,i}^{(n)} + \beta_{ki}u_{k,j}^{(n)} + (n+1)(\delta_{2i}\beta_{kj}u_k^{(n+1)} + \delta_{2j}\beta_{ki}u_k^{(n+1)})].$$

The n th order incremental surface traction $p_i^{(n)}$ is defined as

$$p_i^{(n)} = \beta_{ik}u_j t_{kj}^{(n)} \quad \text{on } C, \quad (12)$$

where C denotes the curve edged the plate in x_1 x_2 plane. The correction factors $\kappa_{(ij)} = \kappa_{(ji)}$ are given by the relations

$$\kappa_{(21)}^2 = \kappa_{(22)}^2 = \kappa_{(23)}^2 = \kappa^2 = \pi^2/12,$$

$$\kappa_{(11)}^2 = \kappa_{(33)}^2 = \kappa_{(13)}^2 = 1.$$

The rotated Y-cuts have the monoclinic symmetry. For the thickness vibrations of these cuts with free edges at $x_1 = \pm a$ we consider straight-crested waves propagating in x_1 direction and retain the two strongly coupled modes, i.e. the thickness-shear $u_1^{(1)}(x_1, t)$ and flexure $u_2^{(0)}(x_1, t)$. The thickness-twist $u_3^{(1)}(x_1, t)$ and thickness-stretch $u_2^{(1)}(x_1, t)$ modes are not coupled with thickness-shear and flexure modes in AT-cut quartz plates and will be not considered in this paper. Hence, by setting $u_1^{(0)} = u_3^{(0)} = 0$ and $t_{11}^{(0)} = t_{13}^{(0)} = t_{33}^{(0)} = 0$ in Eq. (11) and

noting for the rotated Y-cut $\alpha_{12}^0 = \alpha_{13}^0 = \beta_{12} = \beta_{13} = 0$ we have the strain-displacement-temperature relations

$$\begin{aligned} e_{13}^{(0)} &= \frac{1}{2}\beta_4 u_{2,1}^{(0)}, \\ e_{12}^{(0)} &= \frac{1}{2}(\beta_2 u_{2,1}^{(0)} + \beta_1 u_1^{(1)}), \\ e_{11}^{(1)} &= \beta_1 u_{1,1}^{(1)}, \end{aligned} \quad (13)$$

and the free-edge conditions at $x_1 = \pm a$ in the abbreviated notation

$$\begin{aligned} p_2^{(0)} &= \beta_2 t_6^{(0)} + \beta_4 t_5^{(0)} = 0, \\ p_1^{(1)} &= \beta_1 t_1^{(1)} = 0, \end{aligned} \quad (14)$$

where

$$\begin{aligned} \beta_i &= 1 + \alpha_{ii}^0 \quad \text{for } i = 1, 2, 3, \\ \beta_4 &= \alpha_{23}^0. \end{aligned} \quad (15)$$

For the unelectroded plates with the zero traction on the surface the face traction $F_j^{(n)}$ have been set zero. Substitution of Eq. (14) into the first two equations of (10) and (11) yields the incremental-displacement-temperature equations of motion of coupled thickness shear and flexural vibrations. We have in the abbreviated notation of the elastic stiffnesses

$$\begin{aligned} &\kappa^2(\beta_2^2 D_{66} + 2\kappa^{-1}\beta_2\beta_4 D_{56} + \kappa^{-2}\beta_4^2 D_{55})u_{2,11}^{(0)} \\ &+ \kappa^2(\beta_1\beta_2 D_{66} + \kappa^{-1}\beta_1\beta_4 D_{56})u_{1,1}^{(1)} = \varrho \ddot{u}_2^{(0)}, \\ &\beta_1^2 D_{11} u_{1,11}^{(1)} - 3b^{-2}\kappa^2[(\beta_1\beta_2 D_{66} \\ &+ \kappa^{-1}\beta_1\beta_4 D_{56})u_{2,1}^{(0)} + \beta_1^2 D_{66} u_1^{(1)}] = \varrho \ddot{u}_1^{(1)}. \end{aligned} \quad (16)$$

For an even distribution of shearing strain over the face of rotated Y-cut plate, we consider

$$u_2^{(0)} = A_0 b \sin(\xi x_1) e^{i\omega t}, \quad u_1^{(1)} = A_1 \cos(\xi x_1) e^{i\omega t}, \quad (17)$$

where ξ is the wave number and A_0, A_1 are amplitudes.

After substitution of Eq. (17) into Eq. (16) we find

$$\begin{bmatrix} a_{00}z^2 - 3\Omega^2 & a_{01}z \\ a_{01}z & a_{11}z^2 + \hat{a}_{11} - \Omega^2 \end{bmatrix} \begin{bmatrix} A_0 \\ A_1 \end{bmatrix} = 0, \quad (18)$$

where

$$\begin{aligned} a_{00} &= \beta_2^2 \bar{D}_{66} + 2\kappa^{-1}\beta_2\beta_4 \bar{D}_{56} + \kappa^{-2}\beta_4^2 \bar{D}_{55}, \\ a_{01} &= \beta_1\beta_2 \bar{D}_{66} + \kappa^{-1}\beta_1\beta_4 \bar{D}_{56}, \\ a_{11} &= \frac{1}{3}\kappa^{-2}\beta_1^2 \bar{D}_{11}, \\ \hat{a}_{11} &= \beta_1^2 \bar{D}_{66}, \end{aligned} \quad (19)$$

and

$$z = \xi b, \quad \Omega = \omega/\omega_1,$$

$$\omega_1^2 = 3\kappa^2 \frac{C_{66}}{\varrho b^2}, \quad \bar{D}_{pq} = \frac{D_{pq}}{C_{66}}. \quad (20)$$

Setting the determinant of coefficients in Eq. (18) equal to zero gives the dispersion relations from which two

roots of $z_m^2(\Omega)$ can be determined

$$z_m^2(\Omega) = \frac{-q \pm \sqrt{q^2 - 4pr}}{2p}, \quad (21)$$

where

$$\begin{aligned} p &= a_{00}a_{11}, \\ q &= a_{00}(\hat{a}_{11} - \Omega^2) - 3\Omega^2 a_{11} - a_{01}^2, \\ r &= -3\Omega^2(\hat{a}_{11} - \Omega^2). \end{aligned} \quad (22)$$

For each root $z = +\sqrt{z_m^2}$ (for $m=1,2$) the ratio of amplitudes $\alpha_m = A_{1m}/A_{0m}$ can be obtained from the relation

$$\alpha_m = -\frac{a_{01}}{a_{11}z_m^2 + \hat{a}_{11} - \Omega^2} z_m. \quad (23)$$

The complete solution of equations of motion are given by the relations

$$\begin{aligned} u_2^{(0)} &= \sum_{m=1}^2 A_{0m} b \sin(\xi_m x_1) e^{i\omega t}, \\ u_1^{(1)} &= \sum_{m=1}^2 A_{0m} \alpha_m \cos(\xi_m x_1) e^{i\omega t}. \end{aligned} \quad (24)$$

Substitution of Eq. (24) into the edge conditions Eq. (14) yields

$$\begin{bmatrix} (a_{00}z_1 + a_{01}\alpha_1)\cos(z_1 a/b) & (a_{00}z_2 + a_{01}\alpha_2)\cos(z_2 a/b) \\ \alpha_1 \sin(z_1 a/b) & \alpha_2 \sin(z_2 a/b) \end{bmatrix} \times \begin{bmatrix} A_{01} \\ A_{02} \end{bmatrix} = 0, \quad (25)$$

The normalized resonant frequency Ω is a function of the length-to-thickness ratio (a/b) and the elastic properties D_{pq} . It can be obtained from the relation

$$\begin{bmatrix} (a_{00}z_1 + a_{01}\alpha_1)\cos(z_1 a/b) & (a_{00}z_2 + a_{01}\alpha_2)\cos(z_2 a/b) \\ \alpha_1 \sin(z_1 a/b) & \alpha_2 \sin(z_2 a/b) \end{bmatrix} = 0. \quad (26)$$

3. Mechanical effect of plating

The equations of motion of the plated crystal plates were derived by Mindlin [5], Tiersten [6] and Suchánek [11].

Let the upper and lower faces of quartz plate be covered with the electric conducting thin isotropic films (electrodes). Let the thickness of the upper electrode be $2b'$ and the lower electrode $2b''$. The material properties of the upper and lower electrodes are expressed by the mass density ϱ' , the planar elastic stiffness γ_{1111}' and the shear elastic stiffness γ_{1313}' .

Let the platings be perfectly conducting and the

electrodes be so thin that the thickness-shear stress-resultants $t_{2j}^{(0)'}$ and $t_{2j}^{(0)''}$ and the flexure stress-couples $t_{ij}^{(1)'}$ and $t_{ij}^{(1)''}$ may be neglected. The electrodes are isotropic and non-zero thermal expansion coefficients are only $\alpha_{ii}^{(0)'}$ ($i=1,2,3$) and nonzero are also only $\beta_{ii}^{(0)'}$. Then the all that remain of the incremental equations of motion of the plating analogous to (10), (11) and (13) are:

(a) for the upper electrode:

$$\begin{aligned}\beta_{22}' F_2^{(0)'} &= 2b' \varrho' \ddot{u}_2^{(0)'}, \\ \beta_{11}' t_{11,1}^{(0)'} + \beta_{11}' F_1^{(0)'} &= 2b' \varrho' \ddot{u}_1^{(0)'}, \\ t_{11}^{(0)'} &= 2b' \gamma_{1111}^{(0)'} e_{11}^{(0)'}, \\ e_{11}^{(0)'} &= \beta_{11}' u_{1,1}^{(0)'}, \\ F_2^{(0)'} &= [t_{22}^{(0)'}]_{-b'}^{+b'} = t_{22}'(b') - t_{22}'(-b'),\end{aligned}\quad (27)$$

(b) for the lower electrode:

$$\begin{aligned}\beta_{22}'' F_2^{(0)''} &= 2b'' \varrho'' \ddot{u}_2^{(0)''}, \\ \beta_{11}'' t_{11,1}^{(0)''} + \beta_{11}'' F_1^{(0)''} &= 2b'' \varrho'' \ddot{u}_1^{(0)''}, \\ t_{11}^{(0)''} &= 2b'' \gamma_{1111}^{(0)''} e_{11}^{(0)''}, \\ e_{11}^{(0)''} &= \beta_{11}'' u_{1,1}^{(0)''}, \\ F_2^{(0)''} &= [t_{22}^{(0)''}]_{-b''}^{+b''} = t_{22}''(b'') - t_{22}''(-b''),\end{aligned}\quad (28)$$

where

$$\gamma_{1111}^{(0)'} = C_{1111}' - \frac{(C_{1122}')^2}{C_{1111}'}.$$

For the plated crystal plates the conditions of continuity of the incremental surface tractions p_1 and p_2 and the displacement on the faces between electrodes and quartz plate have to be considered:

$$\begin{aligned}\beta_{11}' t_{12}'(-b') &= \beta_{11} t_{12}(b), & \beta_{11}' t_{12}'(b'') &= \beta_{11} t_{12}(-b), \\ \beta_{22}' t_{22}'(-b') &= \beta_{22} t_{22}(b), & \beta_{22}' t_{22}'(b'') &= \beta_{11} t_{22}(-b),\end{aligned}\quad (29)$$

$$\begin{aligned}u_1^{(0)'}(-b') &= b u_1^{(1)}(b), & u_1^{(0)''}(b'') &= -b u_1^{(1)}(-b), \\ u_2^{(0)'}(-b') &= u_2^{(0)}(b), & u_2^{(0)''}(b'') &= u_2^{(0)}(-b),\end{aligned}\quad (30)$$

where we suppose that $u_1^{(0)}=0$, and as $p_3=p_3'=p_3''=0$ the surface traction $F_3^{(0)}=0$.

Using Eq. (29), we may express the surface loading $F_2^{(0)'}$ and $F_1^{(0)'}$ of unelectroded crystal in terms of the surface loadings $F_j^{(0)'}$ and $F_j^{(0)''}$ ($j=1,2$) of electrodes given in the last equations of Eqs. (27) and (28). Then the equation of motion of electrodes (the first equation of Eq. (27) and the first equation of Eq. (28)) may be incorporated in the stress equation of motion of unplated crystal (Eq. (10)).

It follows from the third and fourth equations of

Eqs. (11) and (29)

$$\begin{aligned}\beta_{22}' F_2^{(0)'} &= \beta_{22}' t_{22}'(-b') - \beta_{22}' t_{22}'(b''), \\ \beta_{11}' F_1^{(0)'} &= b \beta_{11}' (t_{12}'(-b') + t_{12}'(b'')).\end{aligned}\quad (31)$$

The successive addition and subtraction of the fourth equation of Eq. (30) and the fourth equation of Eq. (31) yield

$$\begin{aligned}t_{22}'(-b') - t_{22}'(b'') &= \hat{F}_2^{(0)} - (F_2^{(0)'} + F_2^{(0)''}), \\ b t_{12}'(-b') + b t_{12}'(b'') &= \hat{F}_1^{(1)} - b(F_1^{(0)'} - F_1^{(0)''}),\end{aligned}\quad (32)$$

where

$$\begin{aligned}\hat{F}_2^{(0)} &= t_{22}'(b') - t_{22}'(-b''), \\ \hat{F}_1^{(1)} &= b t_{12}'(b') + b t_{12}'(-b''),\end{aligned}\quad (33)$$

are the surface loadings on the outer faces of the platings.

From Eqs. (31) and (32) we obtain

$$\begin{aligned}\beta_{22}' F_2^{(0)'} &= \beta_{22}' \hat{F}_2^{(0)} - \beta_{22}' (F_2^{(0)'} + F_2^{(0)''}), \\ \beta_{11}' F_1^{(0)'} &= \beta_{11}' \hat{F}_1^{(1)} - b \beta_{11}' (F_1^{(0)'} - F_1^{(0)''}).\end{aligned}\quad (34)$$

The sum of the first equation of Eq. (27) and the first equation of Eq. (28) and the difference of the second equation of Eq. (27) and the second equation of Eq. (28) yield

$$\begin{aligned}\beta_{22}' F_2^{(0)'} + \beta_{22}'' F_2^{(0)''} &= 2\varrho' (b' \ddot{u}_2^{(0)'} + b'' \ddot{u}_2^{(0)''}), \\ \beta_{11}' F_1^{(0)'} + \beta_{11}'' F_1^{(0)''} &= -\beta_{11}' (t_{11}^{(0)'} - t_{11}^{(0)''})_{,1} \\ &\quad + 2\varrho' (b' \ddot{u}_1^{(0)'} - b'' \ddot{u}_1^{(0)''}).\end{aligned}\quad (35)$$

Substituting Eq. (35) into Eq. (34) and using the continuity of mechanical displacement condition Eq. (30), we find

$$\begin{aligned}\beta_{22}' F_2^{(0)'} &= \beta_{22}' \hat{F}_2^{(0)} - 2b\varrho R \ddot{u}_2^{(0)}, \\ \beta_{11}' F_1^{(0)'} &= \beta_{11}' \hat{F}_1^{(1)} + b \beta_{11}' (t_{11}^{(0)'} - t_{11}^{(0)''})_{,1} - 2b^3 \varrho R \ddot{u}_1^{(1)},\end{aligned}\quad (36)$$

where the mass loading R is equal to

$$R = \frac{\varrho'(b' + b'')}{\varrho b}.$$

Substituting Eq. (36) into Eq. (10), we obtain

$$\begin{aligned}\beta_{22} \tau_{12,1}^{(0)} + \beta_{23} \tau_{13,1}^{(0)} + \beta_{22}' \hat{F}_2^{(0)} &= 2b\varrho(1+R) \ddot{u}_2^{(0)}, \\ \beta_{11} \tau_{11,1}^{(1)} - \beta_{11} \tau_{12}^{(0)} + \beta_{11}' \hat{F}_1^{(1)} &= \frac{2}{3} b^3 \varrho(1+3R) \ddot{u}_1^{(1)},\end{aligned}\quad (37)$$

where

$$\begin{aligned}\beta_{22} \tau_{12}^{(0)} &= \beta_{22} t_{12}^{(0)}, \\ \beta_{23} \tau_{13}^{(0)} &= \beta_{23} t_{13}^{(0)}, \\ \beta_{11} \tau_{11}^{(1)} &= \beta_{11} t_{11}^{(1)} + b \beta_{11}' (t_{11}^{(0)'} - t_{11}^{(0)''}).\end{aligned}\quad (38)$$

From the conditions of the continuity of mechanical

displacement Eq. (30), we obtain

$$e_{11}^{(0)'} = b \frac{\beta'_{11}}{\beta_{11}} e_{11}^{(1)}, \quad e_{11}^{(0)''} = -b \frac{\beta'_{11}}{\beta_{11}} e_{11}^{(1)}. \quad (39)$$

Substituting from the constitutive equations for the unelectroded crystal Eq. (10) and the electrodes Eqs. (27) and (28) and using Eq. (39) we obtain the stress constitutive equations for the plated crystal in the form

$$\tau_{12}^{(0)} = 2b\kappa(\kappa D_{1212}e_{12}^{(0)} + D_{1213}e_{13}^{(0)}),$$

$$\tau_{13}^{(0)} = 2b(\kappa D_{1312}e_{12}^{(0)} + D_{1313}e_{13}^{(0)}),$$

$$\tau_{11}^{(1)} = \frac{2}{3}b^3 \left(D_{1111} + 3 \left(\frac{\beta'_{11}}{\beta_{11}} \right)^2 \frac{b' + b''}{b} \gamma_{1111}^{\Theta'} \right) e_{11}^{(1)}, \quad (40)$$

where

$$\gamma_{1111}^{\Theta'} = \gamma_{1111}^{\Theta} + \gamma_{1111}^{(1)}(\Theta - \Theta_0)$$

and $\gamma_{1111}^{(1)}$ is first order temperature derivatives of planar elastic stiffness of electrodes $\gamma_{1111}^{\Theta'}$.

For traction-free face conditions the face tractions $F_2^{(1)}$ and $F_1^{(1)}$ have been set to zero. The displacement equation of motion of coupled thickness-shear and flexure vibrations of plated Y-cut quartz plates we obtain in the abbreviated notation in the form

$$\begin{aligned} &\kappa^2(\beta_2^2 D_{66} + 2\kappa^{-1}\beta_2\beta_4 D_{56} + \kappa^{-2}\beta_4^2 D_{55})u_{2,11}^{(0)} \\ &+ \kappa^2(\beta_1\beta_2 D_{66} + \kappa^{-1}\beta_1\beta_4 D_{56})u_{1,1}^{(1)} = \varrho(1+R)\ddot{u}_{2,1}^{(0)}, \\ &\beta_1^2 D_{11}^* u_{1,11}^{(1)} - 3b^{-2}\kappa^2[(\beta_1\beta_2 D_{66} + \kappa^{-1}\beta_1\beta_4 D_{56})u_{2,1}^{(0)} \\ &+ \beta_1^2 D_{66} u_{1,1}^{(1)}] = \varrho(1+3R)\ddot{u}_{1,1}^{(1)}, \end{aligned} \quad (41)$$

where for the same thicknesses of upper and lower electrodes ($b' = b''$)

$$D_{11}^* = D_{11} + 6 \frac{b'}{b} \left(\frac{\beta'}{\beta_1} \right)^2 \gamma_{11}^{\Theta'},$$

$$\beta' = \beta'_{11} = \beta'_{22} = \beta'_{33} = 1 + \alpha^{\Theta'} = 1 + \alpha^{(1)'}(\Theta - \Theta_0) \quad (42)$$

and $\alpha^{(1)'}$ is the first order expansion temperature coefficient of electrodes.

The changes in the displacement equation of motion Eq. (41) which cause the plating of the quartz plate is necessary to applied also into Eqs. (18) and (19). The corrected equations have the form

$$\begin{bmatrix} a_{00}z^2 - 3(1+R)\Omega^2 & a_{01}z \\ a_{01}z & a_{11}z^2 + \hat{a}_{11} - (1+3R)\Omega^2 \end{bmatrix} \times \begin{bmatrix} A_0 \\ A_1 \end{bmatrix} = 0, \quad (43)$$

where

$$a_{00} = \beta_2^2 \bar{D}_{66} + 2\kappa^{-1}\beta_2\beta_4 \bar{D}_{56} + \kappa^{-2}\beta_4^2 \bar{D}_{55},$$

$$a_{01} = \beta_1\beta_2 \bar{D}_{66} + \kappa^{-1}\beta_1\beta_4 \bar{D}_{56},$$

$$a_{11} = \frac{1}{3}\kappa^{-2}\beta_1^2 \bar{D}_{11}^*,$$

$$\hat{a}_{11} = \beta_1 \bar{D}_{66}. \quad (44)$$

The corrected values q and r in Eq. (22) are

$$q = a_{00}(\hat{a}_{11} - (1+3R)\Omega^2) - 3(1+R)\Omega^2 a_{11} - a_{01}^2,$$

$$r = -3(1+R)\Omega^2(a_{11} - (1+3R)\Omega^2), \quad (45)$$

where

$$\bar{D}_{11}^* = D_{11}^*/C_{66}.$$

4. Computed and experimentally obtained results

The normalized resonant frequency Ω as a function of the temperature can be computed from the Eq. (26) when the corrected values Eq. (44) are substituted in Eq. (26) and the dependence of β' , β , D_{ij} and D_{ij} given by Eqs. (42), (2), (15), (20), (3) and (42) is considered.

The AT-cut strips fully covered with electrodes on the faces perpendicular to the thickness of the strip were considered by the computation. The circular AT-cut plates with the diameter 9 mm and the resonant frequency approximately 10 MHz and with the electrode diameter 5.2 mm and 2.8 mm were measured. The computed and measured frequency-temperature characteristic of the AT-cut quartz plates with silver electrodes are shown in Fig. 2 Fig. 3. The mass loading of electrodes of the resonators with the frequency-temperature characteristics shown in Fig. 2 was $R = 0.01875$. Three calcu-

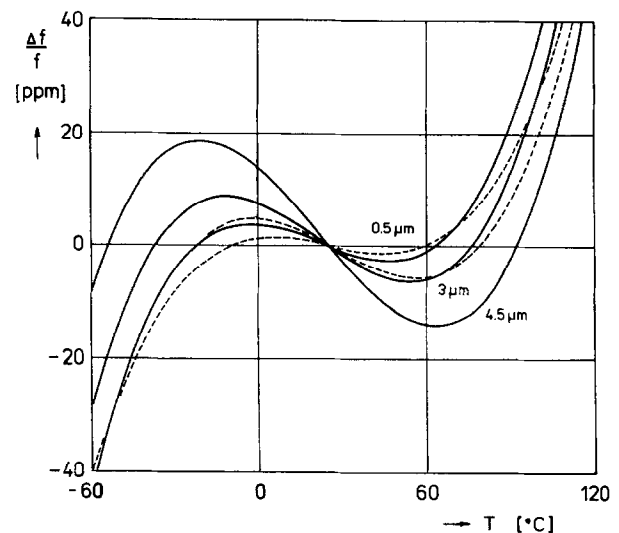


Fig. 2. Calculated (solid line) and measured (dashed lines) frequency-temperature curves of the 10 MHz AT-cut (YXa-35°13,20°) quartz plates.

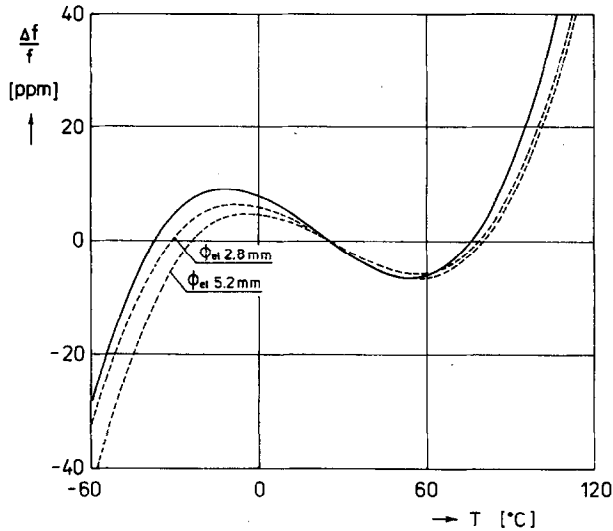


Fig. 3. Calculated (solid lines) and measured (dashed lines) frequency-temperature curves of the 10 MHz AT-cut ($YXa_{-35^\circ 13'/20''}$) quartz plates as a function of the equivalent thickness of silver electrodes. The diameter of electrodes of the measured resonators was 5.2 mm.

lated curves for $R_1=0.003125$, $R_2=0.01875$ and $R_3=0.02813$ and two measured curves for $R_1=0.003125$ and $R_2=0.01875$ are given in Fig. 3. The ratio a/b in the range from 53.77 to 55.20 and the values of material constants of electrodes are given in Table 1.

The resonant frequency of AT-cut quartz resonators as a function of the temperature can be described by the relation

$$\frac{\Omega - \Omega_0}{\Omega_0} = \frac{\Delta\Omega}{\Omega_0} = \sum_{n=1}^3 T f^{(n)}(T - T_0)^n, \quad (46)$$

where Ω is the normalized resonant frequency at the temperature T , Ω_0 is the normalized resonant frequency at the temperature T_0 and $T f^{(n)}$ are n th order temperature coefficients of the resonant frequency.

The influence of the thickness of electrodes caused the change especially the first order temperature coefficient of the resonant frequency. The first order temperature coefficients of the resonant frequency were computed as a function of the mass loading R for the silver and gold electrodes. The computed curves are given in Fig. 4 for three cut angles $35^\circ 12'$, $35^\circ 13'$ and $35^\circ 14'$. The experimental values obtained from the meas-

Table 1

Material constants of electrodes used by the theoretical calculation of the influence of the thickness of electrodes on the frequency-temperature characteristics of resonators

Parameter	Dimension	Silver	Gold
Density	kg m^{-3}	9 300	18 500
Elastic stiffness γ_{11}^p	10^9 N m^{-2}	91.01	92.05
Temperature derivative $\gamma_{11}^{(1)}$	10^9 N m^{-2}	-0.87	-0.68
Thermal expansion coefficient α	10^{-6} K^{-1}	19.7	14.4

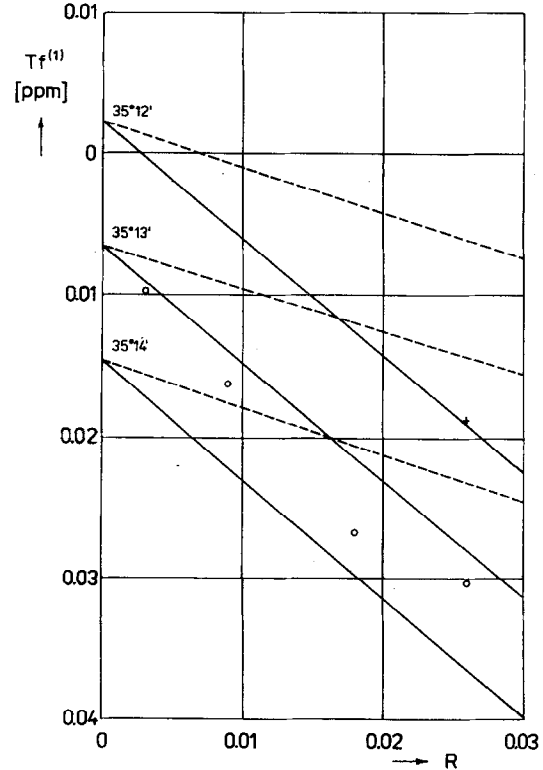


Fig. 4. Calculated dependence of the first order temperature coefficients $T f^{(1)}$ of the AT-cut quartz resonators on the mass loading R for silver (solid line) and gold (dashed lines) electrodes and three cut angles. Circles correspond to the measured values of the AT-cut resonator with silver electrodes and the cross corresponds to the measured values of the same resonator with gold electrodes. The orientation of the measured resonator was $YXa_{-35^\circ 13'/25''}$.

urement of Pavlovec [8] for the AT-cut ($35^\circ 13'/25''$) are also given in Fig. 4.

5. Conclusion

The elastic stiffnesses and inertia of electrodes caused the change of the frequency-temperature characteristic of the AT-cut quartz plates. The value of the first order temperature coefficient of the resonant frequency of the AT-cut quartz resonators decreases linearly with the thickness of electrodes. The silver electrodes caused the greater change of the first order temperature coefficient of the resonant frequency than the gold ones for the same value of mass loading R .

Acknowledgement

The work described here has been funded by the Grant Agency of the Czech Republic, Contract 102/94/1571.

References

- [1] H.F. Tiersten and B.K. Sinha, Proc. 31st AFCF (1977), p. 23.
- [2] D.S. Stevens and H.F. Tiersten, Proc. 34th AFCS (1980), p. 384.
- [3] J.H. Sherman, IEEE Trans. Sonics Ultrason. 30 (1983) 104.
- [4] R.D. Mindlin, An Introduction to the Mathematical Theory of Vibrations of Elastic Plate (US Army Signal Corps Engineering Laboratories, Fort Monmouth, NJ, 1955).
- [5] R.D. Mindlin, in: Progress in Applied Mechanics (Macmillan, New York, 1963) p. 73.
- [6] H.F. Tiersten, Linear Piezoelectric Plate Vibrations (Plenum, New York, 1969).
- [7] P.C.Y. Lee and Y.K. Yong, in: Proc. 38th AFCF (1984), p. 164.
- [8] J. Pavlovic, J. Suchanek and J. Zelenka, in: Proc. 8th Piezoel. Conf. PIEZO'94, Zakopane, Poland (1995), p. 311.
- [9] R. Bechmann, A.D. Ballato and T.J. Lukaszek, Proc. IRE 50 (1962) 1812.
- [10] J.A. Kosinski, J.G. Gualtieri and A. Ballato, IEEE Trans. Sonics Ultrason. Freq. Control 39 (1992) 502.
- [11] J. Suchánek, Ferroelectrics 43 (1982) 17.